SXT CALIBRATION NOTE 37

SXT X-RAY VIGNETTE FUNCTION

R. Fuller, J. Lemen, L. Acton Rev A, 2-Feb-94

1. INTRODUCTION

References: SXT Calibration Notes 1, 4, 18, 36

In this report:

CCDx(F) = CCDx(Flight)
CCDx(L) = CCDx(Lab) (Lab stands for WSMR test data)

and

CCDx(F) = 1049 - CCDx(L)
CCDy(F) = CCDy(L)

Definitions :

Inner-region - The part of the axial-response curve that is due to the objective's X-ray characteristics. This is the region that is within approximately 21 arcmin of the optical axis.

Outer "vignetted" region - The part of the response curve that is a combination of the effects due to the objective's response and due to internal occultation.

2. PROCEDURE AND ANALYSIS OF WSMR DATA

The previous report (Calibration Note 36) established the SXT X-ray axis for the inner-region of the response curve. This was done by assuming the effective area in the inner-region can be described by a linear response function rotated about the optical axis (i.e., a cone). The optical axis was determined by fitting this function to the data by minimizing chi-square. The same assumption and method was used to determine the axis of the outer-region (Lab). These results are shown in Table 1. The units are in CCD full-resolution pixels. The outer-region (Flight) data are discussed below in section 3.

The data analyzed in this report were obtained at the first White Sands Missile Range (WSMR) series of tests in April 1991. The SXT configuration was nearly flight, except, that a different CCD was used, and there were no entrance filters or X-ray analysis filters installed during the calibration.

Table 1: SXT X-ray Optical Axis

	CCDx(F)	CCDy(F)	
Inner-Region	515	633	(See Cal Note 36)
Outer-Region (Lab)	533	599	
Outer-Region (Flight)	530	628	(Adopted)

Once the optical axes are established, it possible to plot all data as a function of distance from the appropriate optical axis and to compare for the different test energies. It was found that the test results could be grouped into two main categories based on the energy of the source. For tests conducted at Al K (1.49 keV) and C K (0.277 keV), the distributions were indistinguishable from one another. However, the distribution obtained with the high energy line Ag L (2.98 keV) had a steeper slope. Because of the different results, the two groups have been designated as "low" energy (for Al K and C K results) and "high" energy (for the Ag L result). The results for both distributions are shown in Figures 1 and 2 which show the effective area as a function of radial position from the center axis.

Upon reviewing the distributions it is clear that the "knee" of the test distributions is at about 17 arcmin. The change in slope at the knee between the inner- and outer-regions may be understood as follows. The slope of the inner-region is due to the optics of the X-ray mirror surfaces. The slope of the outer-region is due to a combination of the optical properties as well as "vignetting" of the source caused by internal occultations of the image from most probably, the filter-rings, but also possibly from other structural baffles and the light baffle cone (located on the front of the filter wheel housing-placed there to reduce the effect of scattered light from large off-axis angles). The point of intersection of these two curves produces the observed "knee" in the response curve.

3. ANALYSIS OF FLIGHT DATA

On a few occasions, the SXT in flight has observed flares in the full-frame images with relatively long exposures. This usually occurs because the spacecraft is unable to change into flare mode, perhaps because of the SAA. During a flare, the data can be badly over-exposed. A good example of this occurred at 6-SEP-92. On some computer systems you may be able to examine two examples using the IDL program SHOW_PIX. Choose the "calibration" subdirectory and look for two files: starb_al01 and starb_almg (short for STAR Burst). If these files do not exist in the show_pix directory, then you may easily create these images by reading the archive tapes.

To create the start burst images, extract the following data:

```
0  6-SEP-92  18:30:00  QT/H  Open /Al.1  Half Norm C  23  2668.0  512x512
1  6-SEP-92  18:48:34  QT/H  Open /Al.1  Half Norm C  23  2668.0  512x512
2  6-SEP-92  18:50:42  QT/H  Open /AlMg  Half Norm C  23  2668.0  512x512
3  6-SEP-92  21:30:54  QT/H  Open /AlMg  Half Norm C  23  2668.0  512x512
```

These images can be found in the files sfr920906.1801 and sfr920906.2116. The Al star burst image can be constructed by the IDL command:

```
starb_al01 = bytscl(alog((sxt_decomp(data(*,*,1)) - sxt_decomp(data(*,*,0)))>1))
```

and the corresponding dagwood image by:

```
starb_almg = bytscl(alog((sxt_decomp(data(*,*,2)) - sxt_decomp(data(*,*,3)))>1))
```

Note carefully which image must be subtracted from the other. The order is reversed between the two filters.

Using a color table that highlights faint detail, one can see a circular feature that corresponds to the knee in Figure 1. Its radius is about 21 arcmin and its center appears at nearly the same place as the outer-region in ground tests: CCDx(F)=530, CCDy(F)=628 (see Table 1).

The discrepancy between the position of the knee in the ground calibration data (17 arcmin) and the flight data (21 arcmin) has been studied in some detail. Since the configuration of the SXT was nearly flight-like (apart from the missing flight filters and final CCD array) the possibility of there existing some piece of flight-hardware that was not present in the ground test situation is very small.

The mostly like explanation depends on the fact that the X-ray source at WSMR was at a finite distance of about 1000 feet. In this case, the angle of the converging beam is slightly shallower, compared to the case where the source is at infinity. By inspecting the internal angles for the cases of an infinite source distance and a finite source distance equal to that of the test situation, two limiting apertures have been determined (see Table2).

Table 2: Calculated limiting Apertures: Two cases

Source Distance	Knee (arcmin)	Filter Wheel (angle in rad)	Light Baffle Cone (angle in rad)	Focal Length (mm)
WSMR (about 1000 ft)	17	0.0005625	0.000574	1526.7
Infinity (flight)	21	0.000600	0.000594	1529.7

Note that in ground test that the Light Baffle Cone is slightly larger than the forward filter wheel ring, but in flight the situation

is reversed. Thus, in the ground tests it may be that the Light Baffle was the limiting aperture, but in the flight the limiting aperture is the filter wheel ring. In principle, with a detailed understanding of all possible limiting apertures, one should be able to predict a change in the knee from 17 arcmin to 21 arcmin between the ground and flight cases. While analysis shows that the trend is the right direction, we are unable to reproduce a shift as large as 4 arcmin.

A close examination of the A101 star burst image (see above) reveals that the feature corresponding to the knee is not perfectly circular. In one place there is a straight section. Thus, our assumption of a cone is not absolutely correct. Furthermore, the possibility that this pattern varies according to flare position in the field-of-view has not been rigorously checked. These issues should be appreciated when analyzing data. (Note: the small-scale cross-cross features are caused by the shadow of the filter mesh. The large spokes are the shadow of the mirror support structure.)

---

4. DISCUSSION AND RESULTS

As described above, there is an unresolved discrepancy in the position of the "knee" in the off-axis response function as determined from pre-launch calibration data and flight data. Since the trend between lab and flight performance is in agreement, we have decided to adopt the flight determination for the position of the knee and to use the slopes as determined from the calibration data. Thus, the assumed mathematical SXT vignette function is the intersection of two non-concentric cones which are given by:

```
Vignette = r_in  * slopein(E)  + B_in(E)     r_in  <= 21 arcmin
Vignette = r_out * slopeout(E) + B_out(E)    r_out >  21 arcmin
```

where E is the energy (either low or high) and

```
r_in  = sqrt( (CCDx(F)-515)^2 + (CCDy(F)-633)^2)
r_out = sqrt( (CCDx(F)-530)^2 + (CCDy(F)-628)^2)
```

The slope and intercept parameters are summarized in Table 3.

As stated in section 3, this is only an approximation to the telescope's true vignette function. In particular, it assumes two non-concentric cones whereas the flight data indicates a deviation from this simple assumption. Only two energies have been investigated and we have not yet determined if the vignette function is dependent on the source position in the SXT field- of-view or not. These limitations should be considered when seeking to correct for the vignette function in SXT images.

Table 3: SXT X-ray Vignette Function Parameters
(Pixel Values refer to full-resolution)

	per pixel	per arcmin	
Low Energy			
B_in(Low)	1.0		
B_out(High)	1.63630		Rcut = 21 arcmin
slopein(Low)	-0.0005085	0.01244	
slopeout(High)	-0.0017472	0.04274	Outer-Region (at r > 21 arcmin)
High Energy			
B_in(Low)	1.0		
B_out(High)	1.20853		Rcut = 21 arcmin
slopein(Low)	-0.0009545	0.02335	Inner-Region (at r <= 21 arcmin)
slopeout(High)	-0.0013605	0.03328	Outer-Region (at r > 21 arcmin)

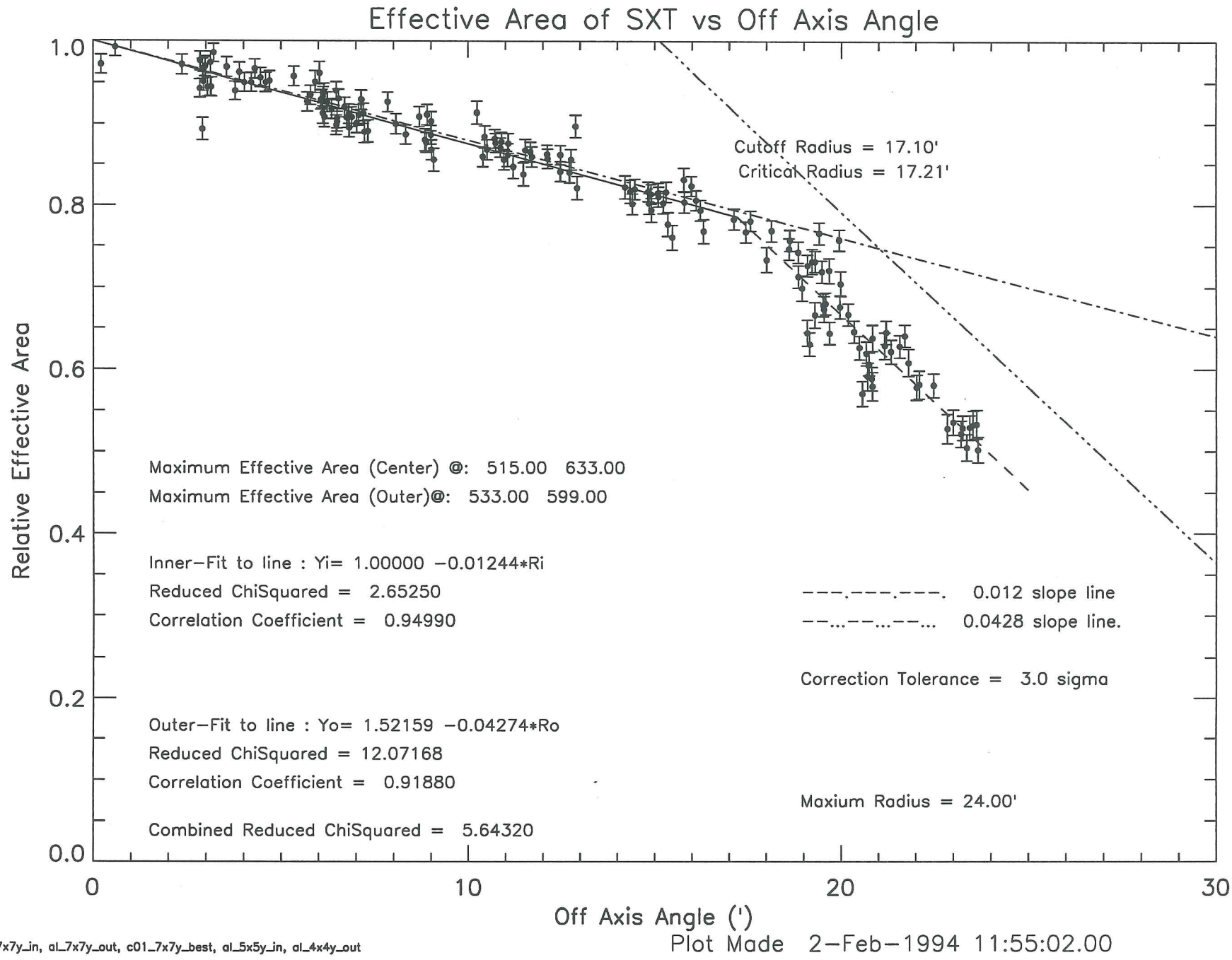

Figure 1. Low energy effective area distribution.

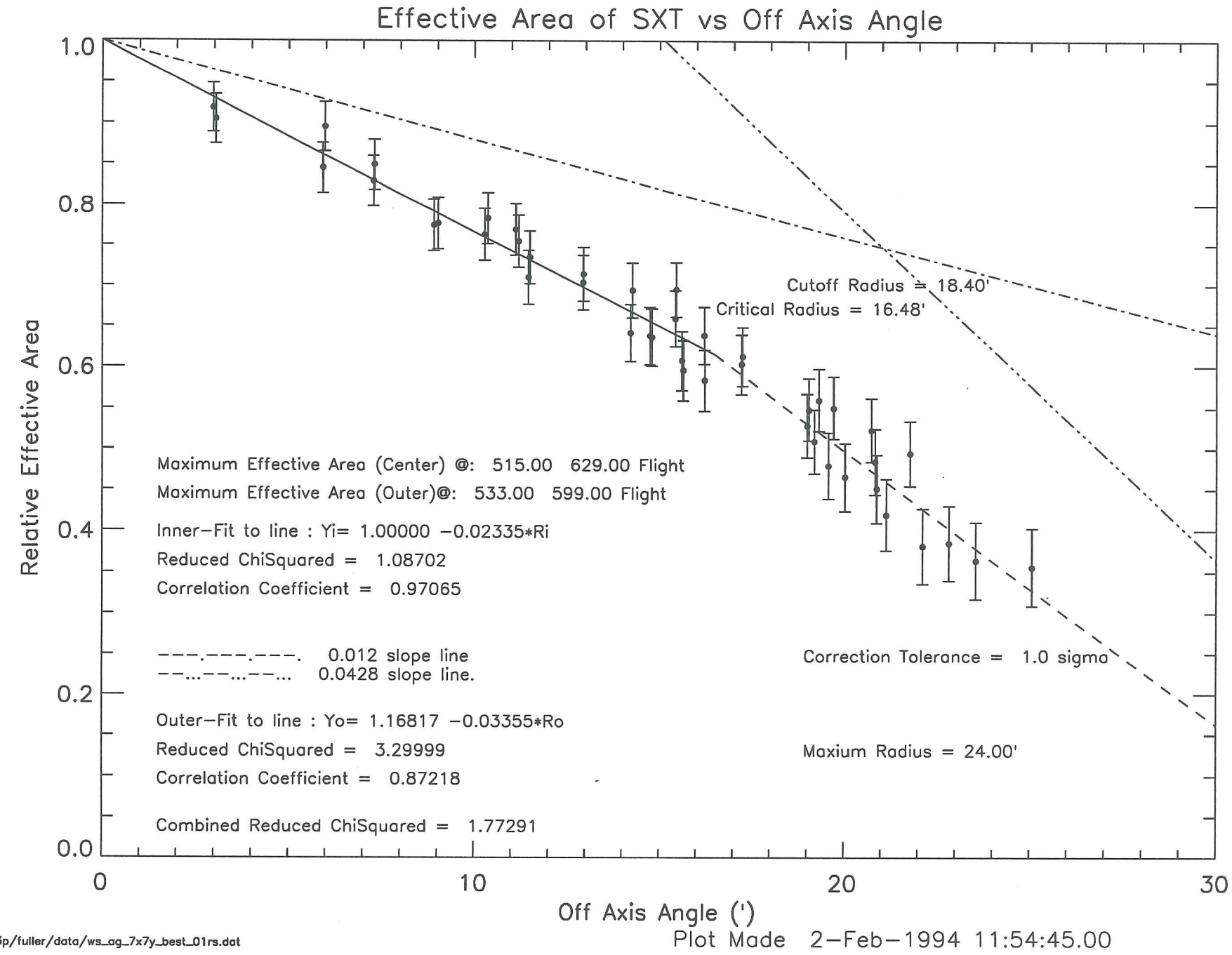

Figure 2. High energy effective area distribution.